MULTIPLE TIME BASE SYCHRONIZATION PROCESS APPLIED TO THE FLIGHT TESTS CAMPAIGN OF A GPS ATTITUDE DETERMINATION ALGORITM

Nelson Paiva Oliveira Leite, PhD.
CTA - Grupo Especial de Ensaios em Vôo
Pça Marechal Eduardo Gomes nº50 (CTA-GEEV)
São José dos Campos, SP, BRAZIL, 12.228-904.
nelson@iae.cta.br

Fernando Walter, PhD.
ITA - Divisão de Eletrônica
Laboratório GNSS
Pça Marechal Eduardo Gomes nº50 (ITA-IEET)
São José dos Campos, SP, BRAZIL, 12.228-900.
fw2@ele.ita.br

ABSTRACT

For the final evaluation of a GPS attitude determination algorithm, it was determined its true performance in terms of its accuracy, reliability and dynamic response. To accomplish that, a flight test campaign was carried out to validate the attitude determination algorithm. In this phase, the measured aircraft attitude was compared to a reference attitude, to allow the determination of the errors. The system was built using non-dedicated THALES Z-FX airborne GPS receivers and a complete Flight Tests Instrumentation (FTI) System. Each GPS receiver operates synchronized with its internal time base. The FTI measurements are synchronized to an IRIG-B time base. All time bases have their own random walk characteristic. To avoid C/A code ambiguity, when its internal time base approaches ±1ms error from the GPS time, its clock is then corrected causing time and phase observables discontinuities. A multiple time base synchronization process was developed to correlate GPS and FTI data. The results are presented and the residual errors were considered acceptable. These data allowed the determination of the performance and accuracy of the GPS attitude determination algorithm. The tests profiles are fully compliant with the Federal Aviation Administration (FAA) Advisory Circular (AC) 25-7A.

KEY WORDS

Attitude, GPS, Flight Tests, Time Correlation, IRIG-B.

INTRODUCTION

The aircraft attitude is the angular relationship between the aircraft body reference system S_B and the local vertical reference system S_R, that can be expressed by the Euler angles: θ (pitch), ϕ (roll), and ψ (yaw). The measurement transformation from S_R to S_B is achieved by three sequential rotations over the Euler angles, for instance the sequence: $[\theta\ \phi\ \psi]$. It is then possible to express a transformation matrix (L_B^R), from S_R to S_B [1] as:

$$L_B^R = \begin{bmatrix} c\theta.c\psi & c\theta.s\psi & -s\theta \\ s\phi.s\theta.c\psi - c\phi.s\psi & s\phi.s\theta.s\psi + c\phi.c\psi & s\phi.c\,\theta \\ c\phi.s\theta.c\psi + s\phi.s\psi & c\phi.s\theta.s\psi - s\phi.c\psi & c\phi.c\theta \end{bmatrix} \tag{1}$$

Where $c\theta \equiv cos(\theta)$, $s\theta \equiv sin(\theta)$, $c\phi \equiv cos(\phi)$, $s\phi \equiv sin(\phi)$, $c\psi \equiv cos(\psi)$, and $s\psi \equiv sin(\psi)$.

The GPS attitude determination algorithm uses two baselines (a_1, a_2) plus a computed baseline (a_3) to define S_G a GPS Cartesian coordinate system, (x_G, y_G, z_G), fixed on the aircraft body, through the installation of three antennas (Ant_1; Ant_2; and Ant_3) [2].
Given an aircraft attitude, it is possible to express the relationship between s_{iR}, a unit vector in the direction of the i^{th} GPS satellite in S_R, and Φ_{jj}, the projection of s_{iR} on the baseline a_j [3], as:

$$\Phi_{ji} = a_j^T L_G^R s_{iR} \tag{2}$$

Where: L_G^R is the Transformation Matrix from S_G to S_R.

Considering that there may be errors in the measured Euler angles (θ_m ϕ_m ψ_m), eq. 3 is not satisfied. So, it is possible to define a cost function (ρ) [4], which is dependent of the transformation matrix (L_G^R):

$$\rho\left(L_G^R\right) = k \sum_{i=1}^{n} p_i \sum_{j=1}^{3} \left| \Phi_{ji} - a_j^T L_G^R s_{iR} \right|^2 \tag{3}$$

Where k is a given coefficient, n is the number of satellites in track, and p_i is a fixed weight value attributed to the i^{th} satellite. The attitude determination algorithm, using least square techniques, searches the transformation matrix (L_G^R) that minimizes ρ. The estimation of the z-axis measurement is given by:

$$\Phi_{3i} = \sqrt{\left(1 - \Phi_{1i}^2 - \Phi_{2i}^2\right)} \tag{4}$$

THE GPS ATTITUDE DETERMINATION ALGORITM (GADA)

When the aircraft is maneuvering, for a given attitude the angle formed by the i^{th} satellite line of sight (LOS_i) and the GPS antenna array horizontal plane (**HAP**) could be negative (i.e. LOS_i is below **HAP**) while the signal received from this satellite is still tracked by the receiver. When this condition occurs, known published GPS attitude determination algorithm attitude output (e.g. REQUEST) diverges from its true value, because eq. 5 computed measurement has a wrong sign.

Then, to minimize the attitude errors build up due to this effect [5], a novel GPS attitude determination algorithm (GADA) was developed and evaluated against a traditional GPS attitude determination algorithms.

To evaluate GADA's performance an attitude reference, provided by a Flight Tests Instrumentation (FTI), was integrated in the Test Aircraft. The FTI System (Figure 01) was composed by an Airborne PCM data acquisition System, a PCM Tape Recorder, an IRIG-B Time Base [6] and a set of Transducers.

Due to equipment availability, it was used a set of independent GPS receivers. For system simplicity, all GPS Observables required for GADA (i.e. Phase, GPS Time, Pseudorange and Ephemeris) were merged into the PCM data stream through a RS232 interface (Figure 02).

This architecture caused some synchronization constraints as follows:

1. For each GPS receiver, its time base is not synchronized with the true GPS time. Time correction occurs only when the time difference reaches 1ms;
2. FTI Time Base (IRIG-B) is not synchronized with the true GPS time;
3. FTI data acquisition uses PCM protocol, so the knowledge of the exact sample time of all measurement, provided by the transducers, is known based on the IRIG Time;
4. GPS observables are merged into the PCM stream, through an asynchronous channel (RS-232). In this case, sample location into the PCM format, does not reflects the sampling time.

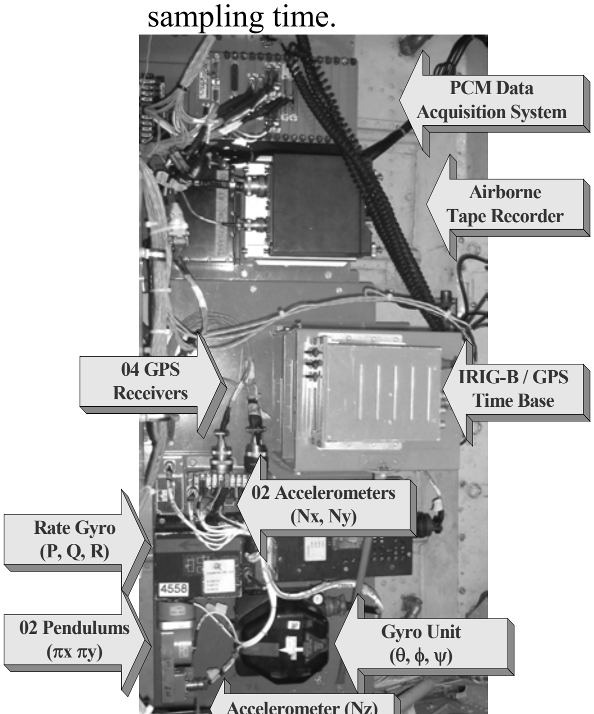

Figure 01 - FTI Installed on the Test Bed

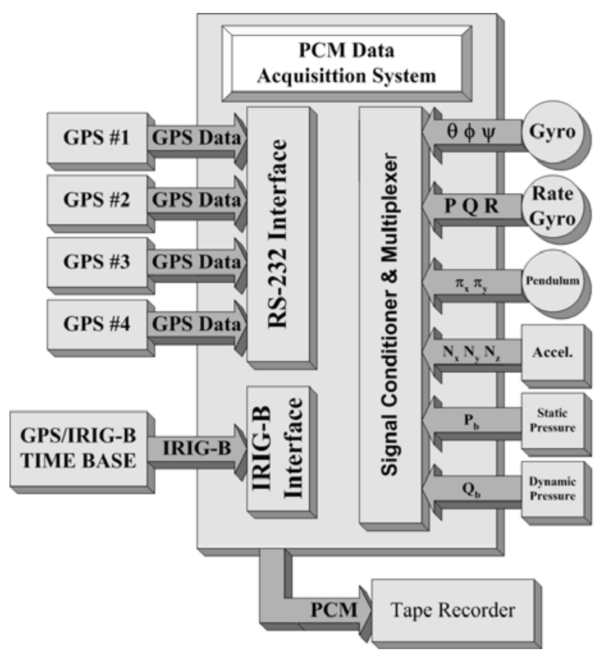

Figure 02 - FTI Block Diagram

All these constraints combined together, jeopardize the GPS attitude determination, as well the evaluation of GADA's Static and Dynamic performance. To overcome these issues, it was developed a synchronization process that works along with a data correction algorithm. This tool was customized to address specific issues related to:

1. The GPS receivers; and
2. The FTI measurements.

GPS RECEIVERS SYNCHRONIZATION

A GPS receiver, computes the raw pseudorange and phase measurements of all in-view satellites synchronized with a 1ms time-tick (i.e. receiver epoch rate), which is generated by the receiver internal clock reference (t_{ri}). Very high accuracy applications, such as attitude determination, seek for true geometric range $R_{Rxi}^{SVj}(t)$ (eq.5) between the j^{th} Satellite Vehicle (SVj) and the i^{th} GPS Receiver (Rxi).

$$R_{Rxi}^{SVj}(t) = v.(t_{ri} - t_t^{SVj}) + \varepsilon_{SVj} \tag{5}$$

Where:

- t_{ri} is the GPS time that the signal was received by Rxi (s);
- t_t^{SVj} is the GPS time that the signal was transmitted by SV_j (s);
- v is the mean propagation speed between SVj and Rxi (m/s); and
- ε_{SVj} is the pseudorange uncertainty (m).

Considering that t_{ri} and t_t^{SVj} are not synchronized with the GPS time, the measured pseudorange (P_{Rxi}^{SVj}) and phase data contains errors (eq. 6).

$$P_{Rxi}^{SVj}(t) = R_{Rxi}^{SVj}(t) + v.(\Delta t_{Rxi} - \Delta t^{SVj}) + \varepsilon_{SVj} \tag{6}$$

Where:

- Δt_{Rxi} is the i^{th} receiver clock error (s); and
- Δt^{SVj} is the j^{th} satellite clock error (s);

The satellite clock error contains two components [7]: the satellite clock drift (Δt_{ck}^{SVj}) and the relativistic effects (Δt_{rel}^{SVj}) and its given by:

$$\Delta t^{SVj} = \Delta t_{ck}^{SVj} + \Delta t_{rel}^{SVj} \tag{7}$$

A 2nd degree polynomial models the satellite clock drift (eq. 8). Its coefficients (a_o, a_1 and a_2) and validity period (T_{oc}^{SVj}) are transmitted embedded into the ephemeris data.

$$\Delta t_{ck}^{SVj} = a_0 + a_1\left(t_{ri} - \frac{P_{Rxi}^{SVj}}{c} - t_{oc}^{SVj}\right) + a_2\left(t_{ri} - \frac{P_{Rxi}^{SVj}}{c} - t_{oc}^{SVj}\right)^2 \tag{8}$$

Where:

c is the GPS speed of light, ***2.99792458 x 10^8*** (m/s);

The relativistic error (eq. 9) is caused by the relative dynamics between the satellite and the receiver [8]. Its minimization algorithm, should know the receiver and the satellite position, as well its orbital parameters.

$$\Delta t_{rel}^{SVj} = F.e.\sqrt{A}.\text{sen}(f_i) \tag{9}$$

Where:

F equals to ***-4,442807633 x 10^-10*** (s/m$^{1/2}$);
e is eccentricity of the orbit (dimensionless);
A is the semi major axis (m); and
f_i is the true orbit anomaly (semicircles);

If the pseudorange and phase errors are negligible, the receiver clock error (Δt_{Rxi}) and the user position ($x_{Rxi}, y_{Rxi}, z_{Rxi}$) can be estimated by a set of equations of at least four in-view satellites, given by:

$$\left.\begin{aligned}
P_{Rxi}^{SV1}(t) &= \sqrt{(x_{SV1}-x_{Rxi})^2+(y_{SV1}-y_{Rxi})^2+(z_{SV1}-z_{Rxi})^2}+v\Delta t_{Rxi}\\
P_{Rxi}^{SV2}(t) &= \sqrt{(x_{SV2}-x_{Rxi})^2+(y_{SV2}-y_{Rxi})^2+(z_{SV2}-z_{Rxi})^2}+v\Delta t_{Rxi}\\
P_{Rxi}^{SV3}(t) &= \sqrt{(x_{SV3}-x_{Rxi})^2+(y_{SV3}-y_{Rxi})^2+(z_{SV3}-z_{Rxi})^2}+v\Delta t_{Rxi}\\
P_{Rxi}^{SV4}(t) &= \sqrt{(x_{SV4}-x_{Rxi})^2+(y_{SV4}-y_{Rxi})^2+(z_{SV4}-z_{Rxi})^2}+v\Delta t_{Rxi}
\end{aligned}\right\} \tag{10}$$

Where:

$x_{SVj}, y_{SVj}, z_{SVj}$ are respectively the estimated $\boldsymbol{x}$, $\boldsymbol{y}$ and $\boldsymbol{z}$ position of the $\boldsymbol{j^{th}}$ satellite (m).

Considering that $\boldsymbol{v}$ is also unknown, a new model for the pseudorange is employed considering that the electromagnetic signal travels at constant speed ($\boldsymbol{c}$). Thus:

$$P_{Rxi}^{SVj}(t) = R_{Rxi}^{SVj}(t) + c.(\Delta t_{Rxi} - \Delta t^{SVj}) + I_{Rxi,SVj}^{SVj}(t) + T_{Rxi}^{SVj}(t) + d_{Rxi,SVj}(t) + d_{Rxi,SVj}^{SVj}(t) + M_{Rxi}^{SVj}(t) + \varepsilon_{SVj} \tag{11}$$

Where:

$I_{Rxi,SVj}^{SVj}$ is the ionosphere delay between $\boldsymbol{SV_j}$ and $\boldsymbol{Rx_i}$ (m);
T_{Rxi}^{SVj} is the troposphere propagation delay between $\boldsymbol{SV_j}$ and $\boldsymbol{Rx_i}$ (m);
$d_{Rxi,SVj}$ is the receiver code error $\boldsymbol{Rx_i}$ (m);
$d_{Rxi,SVj}^{SVj}$ is the satellite code error $\boldsymbol{SV_j}$ (m); e
M_{Rxi}^{SVj} is the multipath error (m).

To minimize these errors, a differential GPS technique computes the single (eq. 13) and double (eq. 14) differences [9], where a baseline is formed between a base and a rover GPS receiver.

Considering a short baseline length (e.g. 100km), most of the propagation effects can be modeled as systematic errors to both receivers (base and rover) and can be minimized.

$$P_{Rx1,Rx2}^{SVj}(t) = R_{Rx1,Rx2}^{SVj}(t) + c.(\Delta t_{Rx1,Rx2}) + M_{Rx1,Rx2}^{SVj}(t) + \varepsilon_{Rx1,Rx2} \quad (12)$$

Where:

$\Delta t_{Rx1,Rx2}$ is the receiver clock error between Rx_1 and Rx_2 (s);

$M_{Rx1,Rx2}^{SVj}$ is the SV_j multipath difference between Rx_1 and Rx_2 (m); and

$\varepsilon_{Rx1,Rx2}$ is the single difference uncertainty between Rx_1 and Rx_2 (m).

$$P_{Rx1,Rx2}^{SVj,SVr}(t) = R_{Rx1,Rx2}^{SVj}(t) - R_{Rx1,Rx2}^{SVr}(t) + M_{Rx1,Rx2}^{SVj,SVr}(t) + \varepsilon_{Rx1,Rx2}^{SVj,SVr} \quad (13)$$

Where:

$M_{Rx1,Rx2}^{SVj,SVr}$ is the multipath residual error from SV_j and SV_r to respectively Rx_1 and Rx_2 (m);

$\varepsilon_{Rx1,Rx2}^{SVj,SVr}$ is the double difference uncertainty between Rx_1 and Rx_2 (m).

A typical GPS receiver uses a linear simplification of eq. 11 [11], to compute its clock error and interactively feedback such results, to refine its time and user position solutions. In fact, some receivers, such as the one used in this work, corrects its internal clock only when Δt_{Rxi} reaches ±1ms threshold (Figure 2), avoiding C/A code ambiguity.

Phase measurements offers better accuracy as compared to pseudorange, so when a receiver has a clock jump (±1ms), the resulting phase double difference contains discontinuities and are unusable for applications such as attitude determination (Figure3).

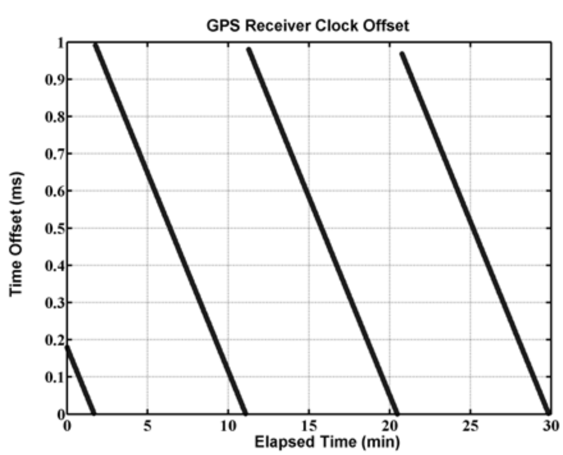

Figure 03 - GPS Receiver Clock Offset

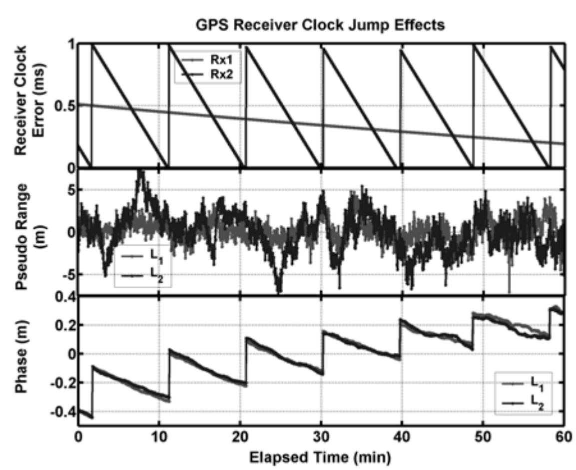

Figure 04 - Clock Jump Effect

Considering no relativistic errors, using the measured ephemeris, phase and pseudorange for all in-view satellites and the receiver computed position and time estimations, the receiver synchronization algorithm performs the following steps:

1. Computes the satellite position, satellite to user geometry and the relativistic error;
2. Computes corrected user position and clock error;
3. Correct pseudorange and phase measurements;
4. Returns to step 1 until algorithm convergence; and
5. Computes single and double differences;

Upon the convergence of this algorithm, it can be found the correct GPS time (T_{GPSi}), when each receiver performed its measurement (eq. 14).

$$T_{GPSi} = t_{Rxi} - \Delta t_{Rxi} \tag{14}$$

In this case, the pseudorange (P_{Rxi}^{SVj}) and phase measurements (Φ_{Rxi}^{SVj}), provided by the receivers that form the antenna array are taken at a known GPS time (t_{GPSi}), but they are not necessary synchronized to each other nor to the GPS epoch, because each receiver has its own time correction factor (Δt_{Rxi}).

To correlate measured phase and pseudorange back to the original reference time (t_{Rxi}), which is synchronized with GPS epoch, it was used an interpolation process (eq. 15).

$$\left.\begin{array}{l} P_{Rxi}^{SVj}(t_{Rxi}) = P_{Rxi}^{SVj}(t_{GPSi}) + \Delta P_{Rxi}^{SVj}(\Delta t_{Rxi}) \\ \Phi_{Rxi}^{SVj}(t_{Rxi}) = \Phi_{Rxi}^{SVj}(t_{GPSi}) + \Delta \Phi_{Rxi}^{SVj}(\Delta t_{Rxi}) \end{array}\right\} \tag{15}$$

Now the problem is that the terms P_{Rxi}^{SVj} and Φ_{Rxi}^{SVj} depends of the relative dynamics between the satellite and the user. To estimate the relative trajectory it was used the ephemeris data and the user position, speed and acceleration data provided by the GPS receiver.

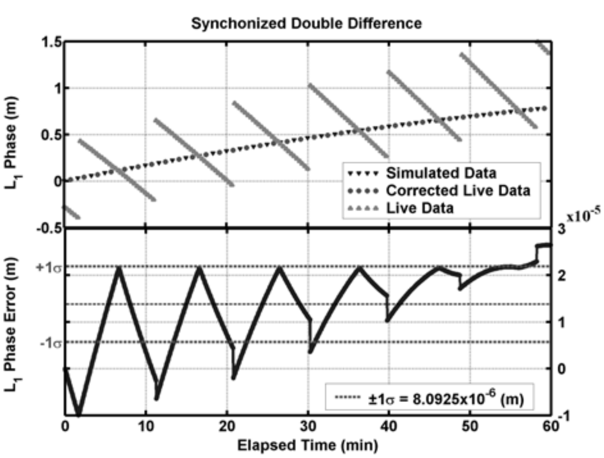

Figure 05 - Phase Interpolation Evaluation

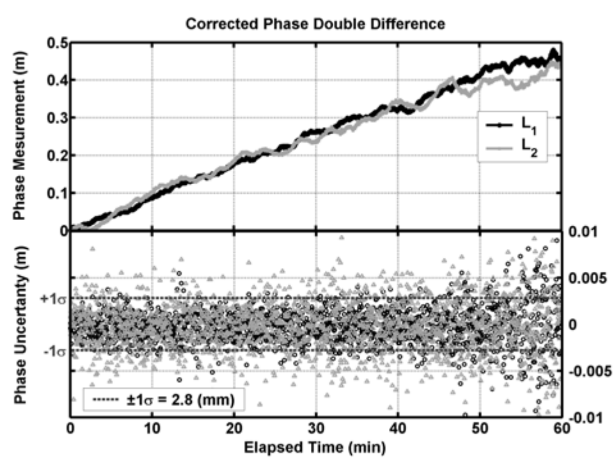

Figure 06 - Live Data Results

The evaluation of the interpolation used a simulation that compared true live data with simulated and corrected data acquired by a fixed baseline. The simulation results were considered satisfactory (Figure 05) and the process was used for real live data (Figure 06).

FTI AND GPS DATA SYNCHRONIZATION

To allow the evaluation of GADA's static and dynamic performance, FTI attitude reference data (θ, ϕ and ψ) should be compared with the GADA's computed attitude solution (θ_G, ϕ_G and ψ_G).

FTI data is measured by an airborne PCM data acquisition system (DAS), that formats sampled data into a synchronous format, so it is possible to know the exact sample time for each parameter, using as reference the IRIG-B time base (t_{FTI}).

GPS embedded data (including t_{Rxi}) is transmitted to the PCM DAS through an asynchronous RS-232 interface, so the exact IRIG-B sampling time (t_{FTI}) of the GPS observables is not known.

To synchronize FTI with the GPS all characters received at the RS-232 input buffer was stamped with IRIG-B time.

Considering negligible the delay between the GPS sampling to the output of the first RS232 character (i.e. **$** string), it was possible to compare the stamped IRIG-B time of the received **$** string with the corrected GPS sample time (i.e. T_{GPSi}) for all receivers.

Using this process, it was noticed that the IRIG-B drift was not negligible (Figure 7), so a 2nd order polynomial calibration curve was used, to synchronize the IRIG-B time base to the GPS reference time. Using this process, the remaining residuals were considered acceptable (Figure8).

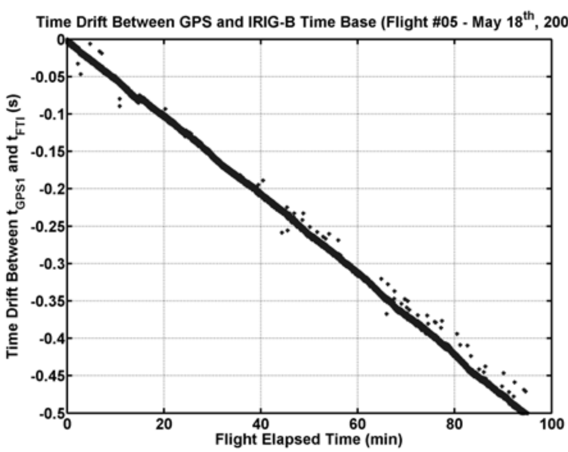

Figure 07 - Time Drift Between GPS and IRIG-B

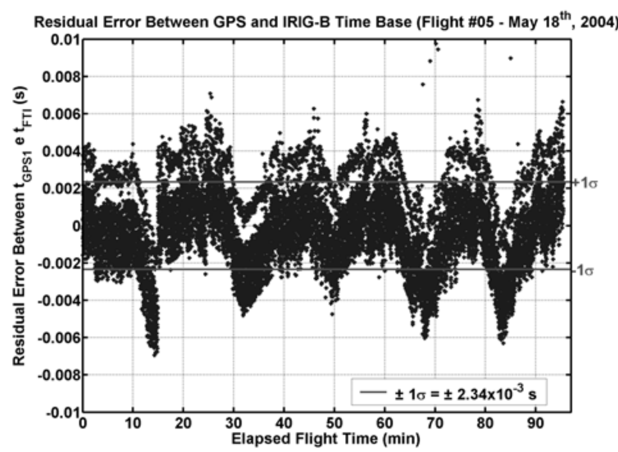

Figure 08 - Live Data Results

With the knowledge of the time drift between FTI and GPS it was possible to interpolate FTI measurement, mainly the FTI attitude, to the GPS sampling time and compare with GADA's solution to determine its errors.

CONCLUSIONS

The synchronization process between the time bases of an array of independent GPS receivers to a PCM FTI IRIG-B time base was developed and tested.

The usage of this methodology enables the interpolation of data, acquired at different sample time, to a unique reference time, allowing the correlation of measurement taken from different sources, and in particular, the evaluation of a novel GPS attitude determination algorithm (GADA) static and dynamic performance.

As example, for the capture of longitudinal attitude maneuver (Figure 09), it was possible to compute the attitude dynamic errors (Figure 10) and using the results to build a dynamic error model [12].

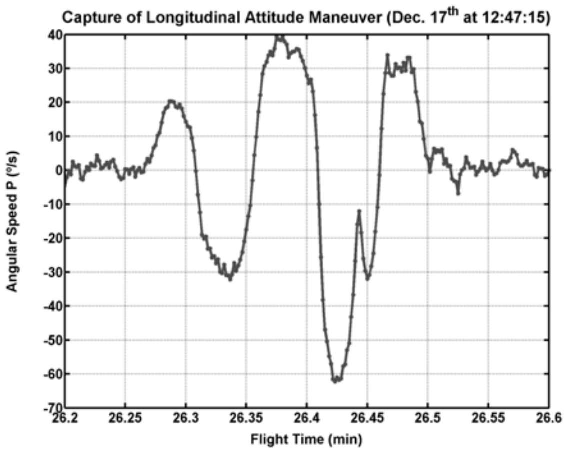

Figure 09 - Capture of Longitudinal Attitude

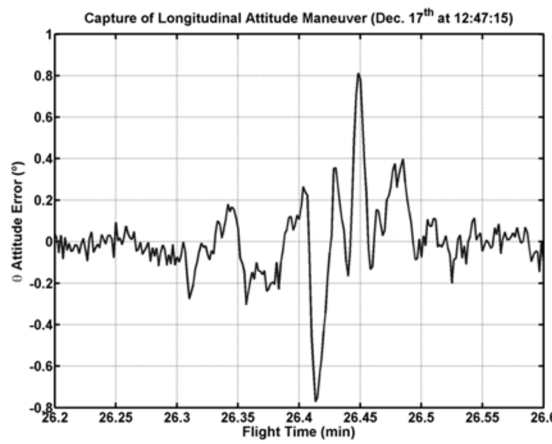

Figure 10 - θ Dynamic Error

Future works should investigate the:

a) Behavior of the methodology with different GPS receivers;
b) The usage of other GPS data acquisition protocols for the FTI (e.g. USB); and
c) The usage of a GPS IRIG-B time base for the FTI system.

ACKNOWLEDGEMENT

We wish to thank the Special Group of Flight Test, for supporting the measurement and the flight tests campaign.

REFERENCES

[1] ETKIN, B. **Dynamics of Atmospheric Flight**. New York: John Willey & Sons, 1972.

[2] COHEN, C. E. Attitude Determination. In: AIAA. **Global Positioning System:** Theory and Applications. Washington: AIAA, 1996, v.2, cap.19, p. 519-537.

[3] SHUSTER, M. D.; OH, S. D. Three-axis Attitude Determination from Vector Observations. **IEEE Journal of Guidance and Control**, Washington, v. 4, n.1, p. 70-77, 1981.

[4] BAR-ITZHACK, I., Y. REQUEST: A Recursive Quest Algorithm for Sequential Attitude Determination. **IEEE Journal of Guidance and Control and Dynamics**, Washington, v.19, n.5, p. 1034-1038, 1996.

[5] LEITE, N. P. O; WALTER, F. The Development and Simulation Results of a GPS Attitude Determination System. In: INSTITUTE OF NAVIGATION NATIONAL TECHNICAL MEETING OF THE SATELLITE DIVISION (ION-GPS), 2002, Portland. **Proceedings …** Portland: ION-GPS, 2002. p. 1100-1107.

[6] INTER-RANGE INSTRUMENTATION GROUP. **IRIG Serial Time Code Formats 200-04**. Secretariat Range Commanders Council: Army White Sands Missile Range, 2004.

[7] SPILKER, J. J. GPS Navigation Data. In: AIAA. **Global Positioning System:** Theory and Applications. Washington: AIAA, 1996, v.1, cap.4, p. 121-176.

[8] ASHBY, N; SPILKER, J. J. Introduction to Relativistic Effects on the Global Positioning System. In: AIAA. **Global Positioning System:** Theory and Applications. Washington: AIAA, 1996, v.1, cap.18, p. 623-697.

[9] LEICK, A. Carrier Phases. In: **GPS Satellite Surveying**. New York: John Willey & Sons, 1995, cap. 8.2, p. 255-264.

[10] KAPLAN, E. D. Position Determination using Pseudorandom Noise (PRN) Codes. In: **Understanding GPS -** Principles and Applications. Norwood: Artech House, 1996, cap. 2.4, p. 39-47.

[11] LEITE, N. P. O.; WALTER, F. Static and Dynamic Performance of a Novel GPS Attitude Determination Algorithm (GADA). In: INSTITUTE OF NAVIGATION NATIONAL TECHNICAL MEETING (ION-NTM), 2007, San Diego. **Proceedings …** San Diego: ION-NTM, 2007. p. 161-171.